Original Article | Breast Imaging

https://doi.org/10.3348/kjr.2017.18.1.238
pISSN 1229-6929 · eISSN 2005-8330
Korean J Radiol 2017;18(1):238-248

Korean Journal of Radiology
KJR

Estimation of T2* Relaxation Time of Breast Cancer: Correlation with Clinical, Imaging and Pathological Features

Mirinae Seo, MD, PhD[1], Jung Kyu Ryu, MD, PhD[2], Geon-Ho Jahng, PhD[2], Yu-Mee Sohn, MD, PhD[1], Sun Jung Rhee, MD, PhD[2], Jang-Hoon Oh, MS[2], Kyu-Yeoun Won, MD, PhD[3]

[1]Department of Radiology, Kyung Hee University Hospital, College of Medicine, Kyung Hee University, Seoul 02447, Korea; Departments of [2]Radiology and [3]Pathology, Kyung Hee University Hospital at Gangdong, College of Medicine, Kyung Hee University, Seoul 05278, Korea

Objective: The purpose of this study was to estimate the T2* relaxation time in breast cancer, and to evaluate the association between the T2* value with clinical-imaging-pathological features of breast cancer.

Materials and Methods: Between January 2011 and July 2013, 107 consecutive women with 107 breast cancers underwent multi-echo T2*-weighted imaging on a 3T clinical magnetic resonance imaging system. The Student's *t* test and one-way analysis of variance were used to compare the T2* values of cancer for different groups, based on the clinical-imaging-pathological features. In addition, multiple linear regression analysis was performed to find independent predictive factors associated with the T2* values.

Results: Of the 107 breast cancers, 92 were invasive and 15 were ductal carcinoma *in situ* (DCIS). The mean T2* value of invasive cancers was significantly longer than that of DCIS (p = 0.029). Signal intensity on T2-weighted imaging (T2WI) and histologic grade of invasive breast cancers showed significant correlation with T2* relaxation time in univariate and multivariate analysis. Breast cancer groups with higher signal intensity on T2WI showed longer T2* relaxation time (p = 0.005). Cancer groups with higher histologic grade showed longer T2* relaxation time (p = 0.017).

Conclusion: The T2* value is significantly longer in invasive cancer than in DCIS. In invasive cancers, T2* relaxation time is significantly longer in higher histologic grades and high signal intensity on T2WI. Based on these preliminary data, quantitative T2* mapping has the potential to be useful in the characterization of breast cancer.

Keywords: *Breast cancer; T2*; Relaxation time; Susceptibility; Breast; Magnetic resonance imaging*

INTRODUCTION

Among all imaging modalities, magnetic resonance imaging (MRI) is the most sensitive method of detecting breast cancer (1-4). Dynamic contrast-enhanced (DCE) MRI is an integral part of the proposed standard protocol for breast cancer diagnosis, which provides important information about temporal and spatial uptake of the contrast medium (5, 6). Recently, research focused on diffusion-weighted imaging, proton spectroscopy, and perfusion MRI, has suggested that these techniques may offer potential improvements for diagnostic breast imaging

Received April 28, 2016; accepted after revision August 20, 2016.
This study was supported by the National Research Foundation (NRF) of Korea grant funded by the Korea government (MSIP) (2014R1A2A2A01002728). The authors would also like to thank Hyug-gi Kim for his technical support of this manuscript.
Corresponding author: Jung Kyu Ryu, MD, PhD, Department of Radiology, Kyung Hee University Hospital at Gangdong, College of Medicine, Kyung Hee University, 892 Dongnam-ro, Gangdong-gu, Seoul 05278, Korea.
• Tel: (822) 440-6188 • Fax: (822) 440-6932 • E-mail: oddie2@naver.com

Korean Journal of Radiology
KJR

(7-12).

Another avenue to help characterize breast lesions is the susceptibility information arising from T2* relaxation. T2* relaxation is the decay of transverse magnetization caused by a combination of spin-spin relaxation and magnetic field inhomogeneity, and includes susceptibility information, which is a unique feature of the tissue (13). Image contrast on susceptibility weighted imaging is affected by paramagnetic deoxyhemoglobin within red blood cells, and is sensitive to the partial pressure of oxygen within vessels (14). Previous studies found that susceptibility information can help to provide information on hypoxia, and to predict the therapeutic response of the tumor. This is of importance since hypoxia is known to reduce the sensitivity towards chemotherapy and radiation therapy (15-19).

In addition to deoxyhemoglobin, static tissue components such as iron deposit, tissue interfaces, or presence of ligamentous/fibrous structures may induce magnetic field inhomogeneity, which causes faster T2* relaxation (i.e., shorter T2* relaxation time), and leads to reduction in signal on gradient-echo (GE) images (13, 20). A recent study showed that the T2* value of the breast glandular tissue is shorter than that of fatty tissue. These results were explained by the magnetic field inhomogeneity of tissue interfaces from fibrocollagenous ligament of Cooper in the glandular tissue, where susceptibility-induced dephasing of proton spins at tissue interfaces can lead to faster T2* relaxation (21).

It is important to understand the relationship between changes of the T2* value of breast cancer and the clinical-imaging-pathological features, because the T2* value might help to provide microstructure information which correlates with magnetic field inhomogeneity. To our knowledge, however, no previous study has included evaluation of the correlation between the T2* value of breast cancer and different clinical-imaging-pathological features. Therefore, the purpose of this study was to estimate the T2* relaxation time of breast cancers, and to evaluate the relationship of the T2* value of breast cancer with clinical-imaging-pathological features.

MATERIALS AND METHODS

Study Population

This study was approved by the Institutional Review Board, and the requirement for informed consent was waived. From January 2011 to July 2013, 190 consecutive patients from a single institution were included, who were diagnosed with breast cancer and underwent breast MRI. Eighty-three patients were excluded from the analysis for the following reasons: 34 patients received neoadjuvant chemotherapy before MRI, 26 had no T2* data, 15 had excisional or vacuum-assisted biopsy before MRI, and 8 did not undergo definitive surgery for breast cancer at our hospital. None of the patients had bilateral breast cancer. In case of multifocal or multicentric cancers, the index cancer was represented by the largest lesion. Finally, 107 women (mean age 52.5 ± 11.3 years, range 29–77) with 107 index breast cancers were analyzed in this study group.

Clinical, Imaging, and Pathological Analysis

Age at diagnosis, menopausal status, symptoms at diagnosis, and family history of breast cancer were obtained from the patient's medical records. Two radiologists (with 12 and 4 years of interpretation of breast images, respectively) reviewed the mammography and MRI in consensus. Mammography determined the breast density and presence of calcifications. In addition, MRI was also reviewed to determine the imaging factors of breast cancers, lesion location, lesion size, and qualitative visual assessment of signal intensity of cancer on T2 weighted image (T2 signal intensity). Lesions were classified into anterior, middle, and posterior location. T2 signal intensity of cancer was compared with that of breast parenchyma on T2-weighted image (T2WI) and classified into three groups: iso-signal intensity, high and very high signal intensity (22). Results of hematoxylin and eosin staining and immunohistochemical staining of the surgical specimen were reviewed. These results determined the tumor pathologic subtype, axillary lymph node status, histologic grade, estrogen receptor (ER), progesterone receptor (PR), human epidermal growth factor receptor 2 (HER2) status, p53, Ki-67, CK 5/6 and molecular subtype. Tumor histologic grade was assessed by the modified Bloom-Richardson scoring system (23). ER-positive and PR-positive tumors were defined by the presence of 1% or more positively stained nuclei at 10 x magnification (24). The staining of c-erb-B2 was scored as 0, 1+, 2+, or 3+. Tumors with a 3+ score were classified as HER2 positive, and tumors with a 0 or 1+ score were classified as negative. In tumors with a 2+ score, gene amplification using fluorescence *in situ* hybridization was used to determine the HER2 status (25). Positive expression of p53 and CK 5/6 was accepted in any case presenting with well-defined nuclear staining. We used

a cutoff value of 14% to divide Ki-67 into high-expression and low-expression groups (26). Regarding molecular subtype, the breast cancers were classified into three groups (hormone receptor [HR]-positive, HER2-positive, and triple-negative), based on the expression of ER, PR, and HER2. HR-positive subtype was defined as either ER- and/or PR-positive/HER2-negative. The HER2-positive subtype was defined to include ER-negative, PR-negative and HER2-positive results. The triple-negative subtype was defined as cancers with ER-negative/PR-negative/HER2-negative results.

MR Imaging Acquisition

All MR examinations were performed with a 3T MRI system (Achieva; Philips Healthcare, Best, the Netherlands) using a four-channel breast coil for reception, with the subject in prone position. At our institute, the regular breast MR imaging protocol included axial T1-weighted image (T1WI), axial short inversion recovery T2WI, axial three-dimensional (3D) DCE-T1WI in both breasts, and 6-minutes delayed, sagittal fat-suppressed, contrast-enhanced T1WI (CE-T1WI) for both breasts. DCE-T1WIs were obtained 20 times with 18.8-second intervals.

To measure T2* relaxation time, a 3D multi-echo GE sequence was acquired with sagittal slices. Seven echo times (TE) were from 2.28 to 25.72 ms in 3.91 ms steps. The imaging parameters were as follows: repetition time = 37.4 ms, flip angle = 20°, field of view = 133 x 130 mm^2, pixel size = 0.55 x 0.55 mm^2, matrix size = 240 x 240, slice thickness = 2.8 mm, the interesting gap = 1.4 mm, number of slices = 105, the number of signals averaged = 1, and sensitivity encoding factor = 1.3. The scan time for T2* mapping was about 4–5 minutes.

Voxel-Based T2* Mapping

To create voxel-based T2* maps, initially seven volumes of the sagittal images were aligned with respect to the first volume to correct any movement. Next, the signals were fitted to obtain S_0 and T2* values, assuming the mono-exponential decay of the signal by using the following equation:

$$S(TE) = S_0 \cdot \exp(-TE / T2^*)$$

where S_0 is the equilibrium signal from the voxel, T2* is the relaxation time, and R2* is the relaxation rate. Using a MATLAB software (Mathworks, Natick, MA, USA), the built-in function *polyfit* was used to fit a linear curve of the logarithmic signal to the TE value for each voxel (18). A T2* value was calculated for each index cancer and normal fibroglandular breast tissue. The CE-T1WI and the first echo GE image were co-registered and resliced to draw regions-of-interest (ROIs) of the breast cancer and the normal

Table 1. Comparison of T2* Values for Cancers and Normal Parenchyma

Tissue Type	No. of Cases	T2* (ms)	*P*
Tissue type			< 0.001
Fibroglandular tissue	107	23.2 ± 8.9	
Invasive cancer	92	30.6 ± 10.9	
Ductal carcinoma *in situ*	15	23.7 ± 7.0	

Fibrogalndular tissue vs. invasive cancer: $p < 0.001$. Fibrogalndular tissue vs. ductal carcinoma *in situ*: $p = 0.981$. Invasive cancer vs. ductal carcinoma *in situ*: $p = 0.029$.

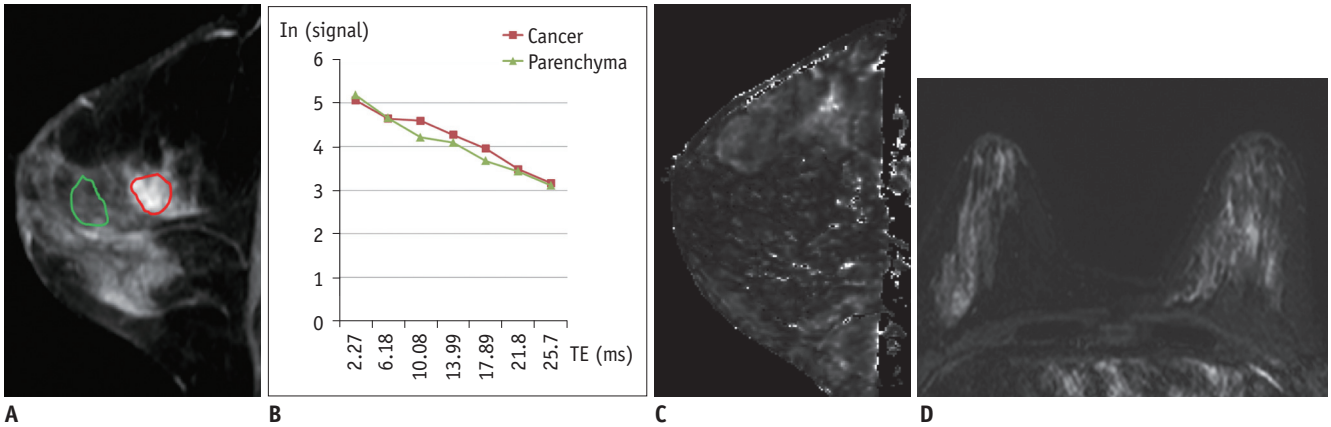

Fig. 1. T2* relaxation time mapping from 55-year-old woman with ductal carcinoma *in situ*.
A. Sagittal contrast-enhanced T1-weighted image shows heterogeneous non-mass enhancement left breast. Region of interest of breast cancer (red) and normal parenchyma (green) was manually outlined and later copied onto T2* map. **B.** Signal intensity changes on MR images were used to calculate intrinsic T2* relaxivity. R2* values were found by taking negative of linear slope of signal intensity plotted against echo time (TE) for each voxel, of which the gradient is–R2* (measured in 1/ms). Reciprocal of R2* was T2*. **C.** T2* map shows similar T2* value in breast cancer compared with surrounding glandular tissue. Mean T2* value of breast cancer and parenchyma were 22.7 and 18.9 ms, respectively. **D.** On coronal T2-weighted image, cancer in left breast was not prominent and classified as iso- signal intensity compared with breast parenchyma.

Korean Journal of Radiology
KJR

parenchyma of the breast. Volumetric ROIs were drawn by one radiologist, having 4 years of experience in breast MR imaging. In order to standardize the lesion analysis as much as possible, the ROI was drawn on the slice in which the cancer showed the greatest diameter, by using a freehand technique in the MRIcro software (http://people.cas.sc.edu/rorden/mricro/index.html). In addition, similar sized ROI were also placed in regions of normal fibroglandular breast tissue in the ipsilateral breast to the known breast cancer. ROIs were drawn on contrast-enhanced MRI to maximize a region of homogeneous tissue type and to avoid large necrotic areas, and later copied onto T2* maps (Fig. 1). The mean T2* values for the two ROIs were obtained for all subjects.

Statistical Analysis

The Student's *t* test and one-way analysis of variance were used to compare T2* values of cancer for different groups based on clinical, imaging and pathological features. Multiple linear regression analysis was performed to find independent predictive factors of cancer associated with T2* values. Only variables with *p* values less than 0.2 at univariate analysis were entered into the multiple regression model. Clinical and imaging features for different groups, according to pathological features, were compared using chi-square and Fisher's exact tests. Two-tailed *p* values < 0.05 were considered statistically significant. Data were analyzed using SPSS version 18 (SPSS Inc., Chicago, IL, USA).

RESULTS

Of the 107 breast cancers, 92 were invasive cancers (72 invasive ductal carcinomas, 10 invasive lobular

Table 2. Clinical and Imaging Features of Invasive Cancer and DCIS

Parameter	Invasive Cancer	DCIS	*P*
Age at diagnosis (years)			0.755
< 45	26 (28.3%)	3 (20.0%)	
≥ 45	66 (71.7%)	12 (80.0%)	
Menopausal status			1.000
Premenopausal	40 (43.5%)	7 (46.7%)	
Postmenopausal	52 (56.5%)	8 (53.3%)	
Symptoms at diagnosis			0.049
Absence	30 (32.6%)	9 (60.0%)	
Presence	62 (67.4%)	6 (40.0%)	
Family history			0.592
Absence	86 (93.5%)	15 (100%)	
Presence	6 (6.5%)	0 (0%)	
Mammographic density			1.000
Fatty	43 (46.7%)	7 (46.7%)	
Dense	49 (53.3%)	8 (53.3%)	
Calcification at mammography			0.233
Absent	65 (70.7%)	8 (53.3%)	
Present	27 (29.3%)	7 (46.7%)	
Location at MRI			0.237
Anterior	10 (10.9%)	0 (0%)	
Middle	47 (51.1%)	11 (73.3%)	
Posterior	35 (38.0%)	4 (26.7%)	
Tumor size at MRI			0.570
< 2.5 cm	58 (63.0%)	8 (53.3%)	
≥ 2.5 cm	34 (37.0%)	7 (46.7%)	
T2 signal intensity at MRI			0.498
Iso-	49 (53.3%)	8 (53.3%)	
High	20 (21.7%)	5 (33.3%)	
Very high	23 (25%)	2 (13.4%)	

Data are numbers of lesions. Values in parentheses are percentages calculated on basis of each group. DCIS = ductal carcinoma *in situ*

Table 3. T2* Values of 92 Invasive Cancers Grouped According to Clinical, Imaging and Pathological Features

Parameter	No. of Cases	T2* Values	*P*
Age at diagnosis (years)			0.972
< 45	26	30.6 ± 9.02	
≥ 45	66	30.7 ± 11.7	
Menopausal status			0.708
Premenopausal	40	30.2 ± 9.2	
Postmenopausal	52	31.0 ± 12.2	
Symptoms at diagnosis			0.342
Absence	30	29.1 ± 10.0	
Presence	62	31.4 ± 11.4	
Family history			0.632
Absence	86	30.5 ± 10.9	
Presence	6	32.7 ± 12.1	
Mammographic density			0.973
Fatty	43	30.7 ± 11.1	
Dense	49	30.6 ± 10.9	
Calcification at mammography			0.061
Absent	65	32.0 ± 11.6	
Present	27	27.3 ± 8.4	
Location at MRI			0.126
Anterior	10	37.0 ± 13.9	
Middle	47	29.3 ± 9.5	
Posterior	35	30.7 ± 11.6	
Tumor size at MRI			0.688
< 2.5 cm	58	30.3 ± 10.8	
≥ 2.5 cm	34	31.2 ± 11.3	
T2 signal intensity at MRI			0.001
Iso-	49	28.0 ± 9.1	
High	20	28.4 ± 8.7	
Very high	23	38.0 ± 13.2	
Pathologic subtype			0.993
IDC + other specific subtype	82	30.6 ± 11.1	
ILC	10	30.7 ± 9.9	
Lymph node metastasis			0.471
Negative	59	31.4 ± 12.4	
Positive	30	29.8 ± 7.9	
Unknown	3		
Histologic grade			0.010
1	16	28.1 ± 8.5	
2	40	28.4 ± 8.8	
3	29	35.9 ± 13.5	
Unknown	7		
ER			0.059
Negative	23	34.4 ± 12.0	
Positive	69	29.4 ± 10.4	
PR			0.099
Negative	33	33.2 ± 11.3	
Positive	59	29.2 ± 10.6	
HER2			0.819
Negative	70	30.8 ± 11.1	
Positive	22	30.2 ± 10.6	

Korean Journal of Radiology
KJR

Table 3. T2* Values of 92 Invasive Cancers Grouped According to Clinical, Imaging and Pathological Features (continued)

Parameter	No. of Cases	T2* Values	*P*
p53			0.108
Negative	27	33.6 ± 9.9	
Positive	64	29.6 ± 11.1	
Unknown	1		
Ki-67			0.090
< 14%	44	28.6 ± 8.9	
≥ 14%	48	32.5 ± 12.3	
CK 5/6			0.215
Negative	37	32.6 ± 9.7	
Positive	53	29.7 ± 11.6	
Unknown	2		
Molecular subtype			0.097
HR-positive	70	29.4 ± 10.3	
HER2-positive	10	32.4 ± 12.4	
Triple-negative	12	36.5 ± 12.3	

CK = cytokeratin, ER = estrogen receptor, HER2 = human epidermal growth receptor 2, HR = hormone receptor, IDC = invasive ductal carcinoma, ILC = invasive lobular carcinoma, PR = progesterone receptor

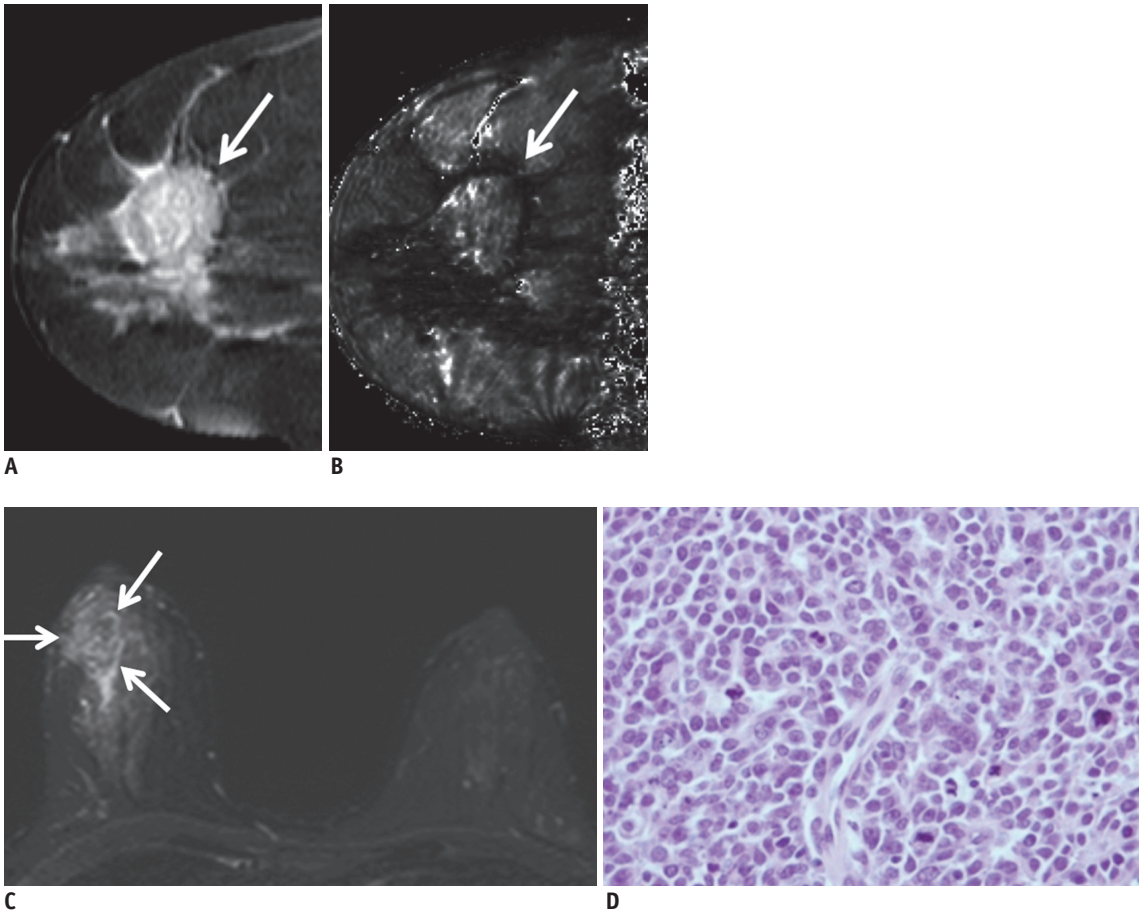

Fig. 2. Representative case in 44-year-old woman with high-grade invasive ductal carcinoma.
A. Sagittal contrast-enhanced T1-weighted image shows heterogeneous enhancing mass (arrow) in right breast middle portion. **B.** T2* map shows increased T2* value in breast cancer (arrow) compared with surrounding glandular tissue. Mean T2* value of breast cancer and normal parenchyma were 50.6 and 35.2 ms, respectively. **C.** Coronal T2-weighted image shows high signal intensity mass accompanying peritumoral edema in right breast (arrows), which was classified as very high signal intensity. **D.** Histopathological image shows high cellularity, no tubule formation, and little collagen matrix (hematoxylin and eosin stain, x 400).

carcinomas, 3 invasive papillary carcinomas, 3 mucinous carcinomas, 2 tubular carcinomas, 1 medullary carcinoma, and 1 metaplastic carcinoma) and the remaining 15 were ductal carcinoma *in situ* (DCIS). The T2* values of the invasive breast cancers were significantly longer than those of the normal glandular tissue ($p < 0.001$) and the 15 cases of DCIS ($p = 0.029$). However, T2* values were not significantly different between DCIS and the normal glandular tissue ($p = 0.981$) (Table 1). Except symptoms at diagnosis, no differences were found in clinical and imaging features between invasive cancer and DCIS groups (Table 2).

Comparisons of T2* values between the sub-groups of the clinical, imaging, and pathological features of 92 invasive cancers are listed in Table 3. In univariate analysis, higher T2 signal intensity of breast cancers as compared with breast parenchyma, showed longer T2* relaxation time ($p = 0.001$). Cancers with higher histologic grade also showed longer T2* relaxation time ($p = 0.01$) (Figs. 2, 3). However, age at diagnosis, menopausal status, symptoms at diagnosis, family history, mammographic density, calcification at mammography, lesion location, and size at MRI, pathologic subtype, lymph node metastasis, ER, PR, HER2, p53, Ki-67, CK 5/6, and molecular subtype did not affect the T2* relaxation time. The T2* values of 92 invasive carcinomas according to each pathologic subtype is shown in Table 4. The first, second, and third longest T2* values were for medullary carcinoma, mucinous carcinoma, and metaplastic carcinoma respectively. The following variables with p values < 0.2 at univariate analysis were entered into the multiple linear regression model: calcification at mammography, lesion location and T2 signal intensity of cancer at MRI, histologic grade, ER, PR, HER2, p53, and Ki-67. In multiple linear regression analysis, the T2 signal intensity ($p = 0.005$) and histologic grade of breast cancer ($p = 0.017$) were significantly associated with T2* relaxation time (Table 5).

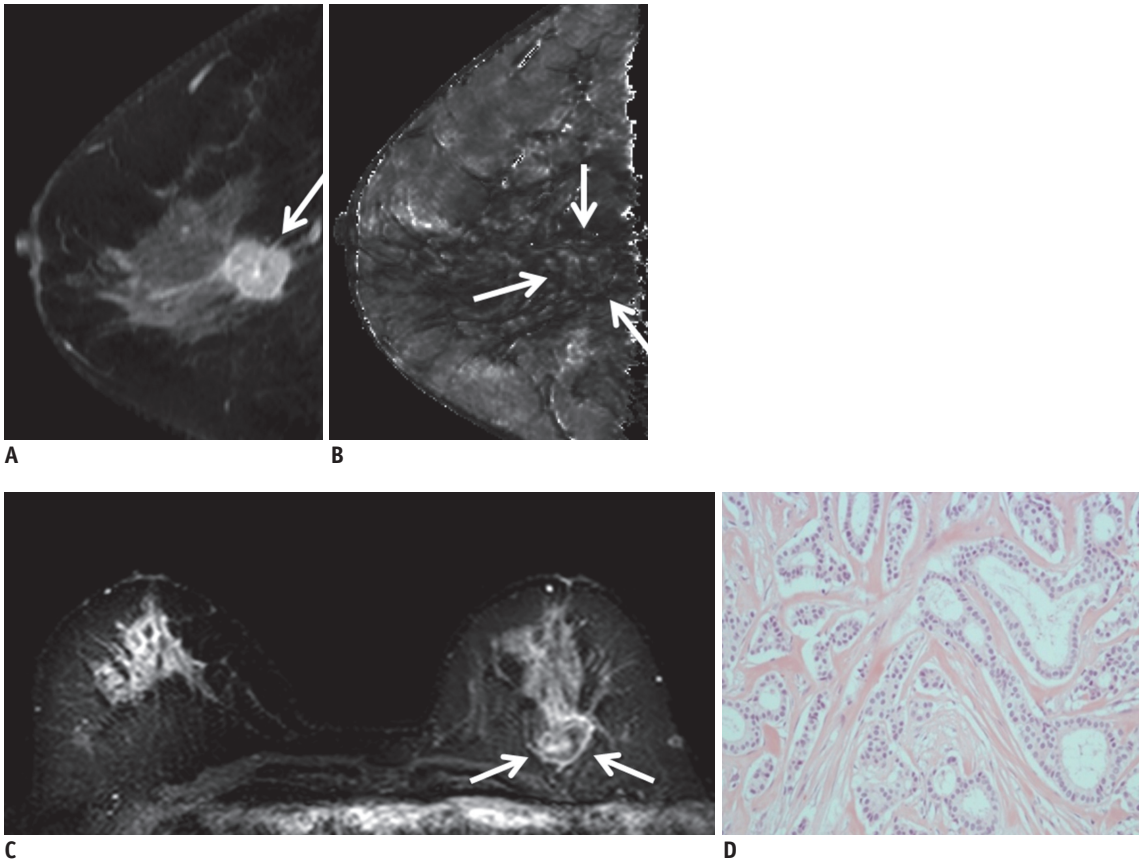

Fig. 3. Representative case in 72-year-old woman with low-grade invasive ductal carcinoma.
A. Sagittal contrast-enhanced T1-weighted image shows posterior located enhancing mass (arrow). **B.** T2* map shows similar T2* value in breast cancer (arrows) compared with surrounding glandular tissue. Mean T2* value of breast cancer and normal parenchyma were 23.4 and 23.4 ms, respectively. **C.** Coronal T2-weighted image shows mass in left breast which is located posterior to breast parenchyma and has slightly higher signal intensity compared to breast parenchyma (arrows). **D.** Histopathological image shows increased tubule and gland formation, and rich collagen matrix (hematoxylin and eosin stain, x 200).

Korean Journal of Radiology
KJR

DISCUSSION

The major finding of this study revealed that T2* values of breast cancers were significantly different between invasive cancers and DCIS. In addition, T2* was significantly longer in the breast cancer group, having a higher T2 signal intensity and higher histologic grade. These results suggested an additional significance of T2* estimation in yielding information of the tumor microstructure.

Our results show that T2* relaxation time of invasive cancer was longer than normal breast tissue ($p < 0.001$). Li et al. (18) reported that the T2* relaxation time was longer in tumor tissue than normal breast tissue, and this result was concordant with our study. The authors expected that the T2* relaxation time of tumor tissue was shorter than breast tissue due to effects of deoxyhemoglobin, but the results were, in fact, opposite. The authors explained their results by the magnetic field inhomogeneity of tissue interfaces from fibrocollagenous ligament of Cooper in the glandular tissue, that overcomes the opposing effects of deoxyhemoglobin (18). Likewise, our result that the T2* value of the invasive breast cancers was longer than that of DCIS ($p = 0.029$) was validated with the above-mentioned results. In DCIS, intact fibroligamentous breast tissue adjacent to the neoplastic epithelial cell proliferations confined to the mammary ductal and lobular systems in ROI, might result in magnetic field inhomogeneity and faster T2* relaxation compared with invasive cancers. Another study of the prostate showed that static tissue components may potentially result in faster T2* relaxation in fibrous tissue within benign prostatic hyperplasia and anterior fibrous band of the prostate (27). In addition, because DCIS was manifested by non-mass enhancement rather than mass, the normal parenchyma adjacent to the enhancing lesion is easily contained within ROI, and may affect the T2* relaxation. Even though there was no statistically significant difference in calcifications at mammography between invasive cancer and DCIS groups, portions of the calcification were higher in DCIS group than in the invasive cancer group. We cannot exclude the possibility that magnetic field inhomogeneity induced by calcification might affect the difference of T2* relaxation between invasive cancer and DCIS.

In our study, T2* relaxation time was longer in higher grade tumor group in both univariate and multivariate analyses. However, according to previous studies which revealed that higher grade tumors had the lowest polarographic O_2 values, it was expected that higher grade tumors would have faster T2* relaxation because of a higher anoxic and hypoxia fraction (28, 29). We presume this paradoxical result might be due to structural differences based on the histologic grade, and these effects presumably overcome the opposing effects of hypoxia. According to a previous study which analyzed the correlation between the tumor-stroma ratio and modified Bloom-Richardson grade (30), stroma-poor breast cancers correlated with high grade cancers, and stroma-rich breast cancer correlated with low grade cancer. We suppose that the static stromal component, including tissue collagen, might induce magnetic field inhomogeneity and result in decreased

Table 4. T2* Values of 92 Invasive Cancers According to Histologic Subtypes

Subtype	No. of Cases	T2* Values (ms)
Invasive ductal carcinoma	72	29.3 ± 9.6
Invasive lobular carcinoma	10	30.7 ± 89.9
Invasive papillary carcinoma	3	31.3 ± 13.0
Mucinous carcinoma	3	49.9 ± 15.8
Tubular carcinoma	2	26.8 ± 10.4
Medullary carcinoma	1	66.4
Metaplastic carcinoma	1	38.5

Table 5. Results of Multiple Linear Regression Analysis to Examine Independent Predictive Factors Associated with T2* Value of 92 Invasive Cancers

Variables	Coefficient (β)	Standard Error*	*P*
Calcification	-4.629	2.443	0.062
Location	-1.281	1.675	0.447
T2 signal intensity	4.042	1.401	0.005
Histologic grade	5.792	2.374	0.017
ER	0.285	3.851	0.941
PR	1.371	3.584	0.703
p53	-3.785	2.684	0.553
Ki-67	-1.876	3.146	0.163

*Standard error of estimated coefficient. ER = estrogen receptor, PR = progesterone receptor

T2* relaxation time in low grade breast cancer, which was characterized by increased tubule and gland formation, low cellularity, and rich collagen matrix (31, 32). Subtype of medullary carcinoma, defined as scant stroma and prominent lymphoid infiltration (33), shows the longest T2* value among the subtype of invasive cancers in our study. A significant correlation between breast tumor T2* relaxation and tumor grade was also reported in another clinical study (34). However, contrary to the observations of our study, Liu et al. (19) showed that the T2* relaxation rate was not correlated with histologic grade. Compared with that study, we evaluated additional factors, T2 signal intensity and presence of calcifications on mammography, which might affect the T2* relaxation.

We analyzed the qualitative visual assessment of cancer compared with parenchyma in T2WI, and correlated them with quantitative T2* mapping. T2* values of invasive cancers showed a significant correlation with T2 signal intensity in both univariate and multivariate analyses. T2* relaxation is a combined effect of true T2 relaxation and relaxation affected by magnetic field inhomogeneities according to the following equation: $1 / T2^* = 1 / T2 + \gamma \Delta Binhom$, where γ is the gyromagnetic ratio and $\Delta Binhom$ is the magnetic field inhomogeneity across a voxel (35). Thus, T2 and T2* parameters in MRI were associated with each other. In our study, T2* relaxation times of mucinous carcinoma and metaplastic carcinoma, known to have a long T2 relaxation time and showing high T2 signal intensity (36, 37), were the 2nd and 3rd longest values respectively among subtypes of invasive cancers. Uematsu et al. (22) reported that tumors with higher degree of fibrosis, mainly collagen fibers present, correlated with low or equal T2 signal intensity. Considering our results that T2* was significantly shorter in breast cancer group with lower histologic grade characterized by rich collagen matrix, collagen fiber might affect T2 relaxation as well as T2* relaxation. In our study, T2* value was still associated with histologic grade when the qualitative T2 effect was corrected. Regarding molecular subtype, even though there was no statistical significance, triple negative group shows longer T2* relaxation than HR-positive subtype in our study, and this result was relatively consistent with a previous study that shows triple negative breast cancer has high or very high T2 signal intensity than other subtypes (22). It is well known that additional information of T2WI can increase the specificity of breast MR imaging (38). Regarding T2* values which reflect susceptibility induced field distortions, only a small number of studies have been performed in breast MR imaging (18, 19). Further studies with large sample size comparing the T2 and T2* values might provide additional helpful information concerning histopathologic characteristics or tumor microstructure.

A number of limitations may affect the applicability of our findings. First, the sample size might be too small to draw a solid conclusion. Second, we did not assess the correlation between quantitative assessment of calcifications of breast cancer and T2* relaxation. We only evaluated correlation between the T2* relaxation time and presence of calcifications on mammography. The cancers with calcifications on mammography showed shorter relaxation time, albeit without statistical significance ($p = 0.062$), and this result might reflect that magnetic field inhomogeneities arise from iron deposits induce faster T2* relaxation. Third, we did not evaluate the correlation between quantitative fibrotic component and the T2* value. Fourth, we did not compare T2* relaxation times of benign tumors and cancer. Further studies which correlate quantitative static tissue component information using special staining for fibrotic component and microcalcifications on surgical specimens are needed to confirm our observations.

In conclusion, we observed that the T2* value was significantly longer in invasive cancer than DCIS. Regarding invasive cancers, T2* relaxation time was significantly longer in cancer with high histologic grade and high signal intensity on T2WI. Based on these preliminary data, T2* estimation may be suggested as a potential tool for yielding information of the breast tumor microstructure.

REFERENCES

1. Kriege M, Brekelmans CT, Boetes C, Besnard PE, Zonderland HM, Obdeijn IM, et al. Efficacy of MRI and mammography for breast-cancer screening in women with a familial or genetic predisposition. *N Engl J Med* 2004;351:427-437
2. Kuhl CK, Schrading S, Leutner CC, Morakkabati-Spitz N, Wardelmann E, Fimmers R, et al. Mammography, breast ultrasound, and magnetic resonance imaging for surveillance of women at high familial risk for breast cancer. *J Clin Oncol* 2005;23:8469-8476
3. Leach MO, Boggis CR, Dixon AK, Easton DF, Eeles RA, Evans DG, et al. Screening with magnetic resonance imaging and mammography of a UK population at high familial risk of breast cancer: a prospective multicentre cohort study (MARIBS). *Lancet* 2005;365:1769-1778
4. Ko ES, Han H, Han BK, Kim SM, Kim RB, Lee GW, et al. Prognostic significance of a complete response on breast MRI

in patients who received neoadjuvant chemotherapy according to the molecular subtype. *Korean J Radiol* 2015;16:986-995
5. Obdeijn IM, Loo CE, Rijnsburger AJ, Wasser MN, Bergers E, Kok T, et al. Assessment of false-negative cases of breast MR imaging in women with a familial or genetic predisposition. *Breast Cancer Res Treat* 2010;119:399-407
6. Pages EB, Millet I, Hoa D, Doyon FC, Taourel P. Undiagnosed breast cancer at MR imaging: analysis of causes. *Radiology* 2012;264:40-50
7. Yoon JH, Kim MJ, Kim EK, Moon HJ. Imaging surveillance of patients with breast cancer after primary treatment: current recommendations. *Korean J Radiol* 2015;16:219-228
8. Huang W, Fisher PR, Dulaimy K, Tudorica LA, O'Hea B, Button TM. Detection of breast malignancy: diagnostic MR protocol for improved specificity. *Radiology* 2004;232:585-591
9. Gruber S, Debski BK, Pinker K, Chmelik M, Grabner G, Helbich T, et al. Three-dimensional proton MR spectroscopic imaging at 3 T for the differentiation of benign and malignant breast lesions. *Radiology* 2011;261:752-761
10. Yabuuchi H, Matsuo Y, Okafuji T, Kamitani T, Soeda H, Setoguchi T, et al. Enhanced mass on contrast-enhanced breast MR imaging: lesion characterization using combination of dynamic contrast-enhanced and diffusion-weighted MR images. *J Magn Reson Imaging* 2008;28:1157-1165
11. Kul S, Cansu A, Alhan E, Dinc H, Gunes G, Reis A. Contribution of diffusion-weighted imaging to dynamic contrast-enhanced MRI in the characterization of breast tumors. *AJR Am J Roentgenol* 2011;196:210-217
12. Seo M, Cho N, Bae MS, Koo HR, Kim WH, Lee SH, et al. Features of undiagnosed breast cancers at screening breast MR imaging and potential utility of computer-aided evaluation. *Korean J Radiol* 2016;17:59-68
13. Chavhan GB, Babyn PS, Thomas B, Shroff MM, Haacke EM. Principles, techniques, and applications of T2*-based MR imaging and its special applications. *Radiographics* 2009;29:1433-1449
14. González Hernando C, Esteban L, Cañas T, Van den Brule E, Pastrana M. The role of magnetic resonance imaging in oncology. *Clin Transl Oncol* 2010;12:606-613
15. Padhani AR, Krohn KA, Lewis JS, Alber M. Imaging oxygenation of human tumours. *Eur Radiol* 2007;17:861-872
16. Busk M, Horsman MR. Relevance of hypoxia in radiation oncology: pathophysiology, tumor biology and implications for treatment. *Q J Nucl Med Mol Imaging* 2013;57:219-234
17. McPhail LD, Robinson SP. Intrinsic susceptibility MR imaging of chemically induced rat mammary tumors: relationship to histologic assessment of hypoxia and fibrosis. *Radiology* 2010;254:110-118
18. Li SP, Taylor NJ, Makris A, Ah-See ML, Beresford MJ, Stirling JJ, et al. Primary human breast adenocarcinoma: imaging and histologic correlates of intrinsic susceptibility-weighted MR imaging before and during chemotherapy. *Radiology* 2010;257:643-652
19. Liu M, Guo X, Wang S, Jin M, Wang Y, Li J, et al. BOLD-MRI of breast invasive ductal carcinoma: correlation of R2* value and the expression of HIF-1α. *Eur Radiol* 2013;23:3221-3227
20. Padhani A. Science to practice: what does MR oxygenation imaging tell us about human breast cancer hypoxia? *Radiology* 2010;254:1-3
21. Ryu JK, Oh JH, Kim HG, Rhee SJ, Seo M, Jahng GH. Estimation of T2* relaxation times for the glandular tissue and fat of breast at 3T MRI system. *JKSMRM* 2014;18:1-6
22. Uematsu T, Kasami M, Yuen S. Triple-negative breast cancer: correlation between MR imaging and pathologic findings. *Radiology* 2009;250:638-647
23. Elston CW, Ellis IO. Pathological prognostic factors in breast cancer. I. The value of histological grade in breast cancer: experience from a large study with long-term follow-up. *Histopathology* 1991;19:403-410
24. Hammond ME, Hayes DF, Wolff AC, Mangu PB, Temin S. American society of clinical oncology/college of american pathologists guideline recommendations for immunohistochemical testing of estrogen and progesterone receptors in breast cancer. *J Oncol Pract* 2010;6:195-197
25. Dolan M, Snover D. Comparison of immunohistochemical and fluorescence in situ hybridization assessment of HER-2 status in routine practice. *Am J Clin Pathol* 2005;123:766-770
26. Cheang MC, Chia SK, Voduc D, Gao D, Leung S, Snider J, et al. Ki67 index, HER2 status, and prognosis of patients with luminal B breast cancer. *J Natl Cancer Inst* 2009;101:736-750
27. Hoskin PJ, Carnell DM, Taylor NJ, Smith RE, Stirling JJ, Daley FM, et al. Hypoxia in prostate cancer: correlation of BOLD-MRI with pimonidazole immunohistochemistry-initial observations. *Int J Radiat Oncol Biol Phys* 2007;68:1065-1071
28. Hohenberger P, Felgner C, Haensch W, Schlag PM. Tumor oxygenation correlates with molecular growth determinants in breast cancer. *Breast Cancer Res Treat* 1998;48:97-106
29. Höckel M, Vaupel P. Tumor hypoxia: definitions and current clinical, biologic, and molecular aspects. *J Natl Cancer Inst* 2001;93:266-276
30. Ko ES, Han BK, Kim RB, Cho EY, Ahn S, Nam SJ, et al. Apparent diffusion coefficient in estrogen receptor-positive invasive ductal breast carcinoma: correlations with tumor-stroma ratio. *Radiology* 2014;271:30-37
31. Elston CW, Ellis IO. Pathological prognostic factors in breast cancer. I. The value of histological grade in breast cancer: experience from a large study with long-term follow-up. Histopathology 2002;41(3A):154-161
32. Lee SH, Cho N, Kim SJ, Cha JH, Cho KS, Ko ES, et al. Correlation between high resolution dynamic MR features and prognostic factors in breast cancer. *Korean J Radiol* 2008;9:10-18
33. Lakhani SR, Ellis IO, Schnitt SJ, Tan PH, van de Vijver MJ. *WHO classification of Tumours of the breast*, 4th ed. Lyon: International Agency for Research on Cancer, 2012:14-31
34. Padhani AR, Ah-See ML, Taylor NJ. *An investigation of histological and DC-MRI correlates of intrinsic susceptibility contrast relaxivity* (R2*) *in human breast cancer*. Berkeley, CA: Proceedings of the Thirteenth Meeting of the International Society for Magnetic Resonance in Medicine, 2005:1846

35. Hendrick RE. *Image contrast and noise*. In: Stark DD, Bradley WG, eds. *Magnetic resonance imaging*, 3rd ed. St Louis, MO: Mosby, 1999:43-68
36. Kawashima M, Tamaki Y, Nonaka T, Higuchi K, Kimura M, Koida T, et al. MR imaging of mucinous carcinoma of the breast. *AJR Am J Roentgenol* 2002;179:179-183
37. Velasco M, Santamaría G, Ganau S, Farrús B, Zanón G, Romagosa C, et al. MRI of metaplastic carcinoma of the breast. *AJR Am J Roentgenol* 2005;184:1274-1278
38. Yuen S, Uematsu T, Kasami M, Tanaka K, Kimura K, Sanuki J, et al. Breast carcinomas with strong high-signal intensity on T2-weighted MR images: pathological characteristics and differential diagnosis. *J Magn Reson Imaging* 2007;25:502-510